Welded-Ag-nanowires/FTO conducting film with high transmittance and its application in transparent supercapacitors

Zhensong Qiao, Xiaopeng Yang[1,*], Feng Liu, Guangbin Duan and Bingqiang Cao[2,*]

Materials Research Centre for Energy and Photoelectrochemical Conversion, School of Material Science and Engineering University of Jinan, Jinan 250022, Shandong, China.

E-mail: [1,*] mse_yangxp@ujn.edu.cn, [2,*] mse_caobq@ujn.edu.cn.

Abstract. Silver nanowires (AgNW)with a small diameter weresynthesized by a facile and novel polyol reduction method. Ag nanowires ink was then spun on the surface of F-doped SnO_2 (FTO) to form the AgNW/FTO conducting film. Welding treatment of the AgNW/FTO conducting film not only increased the optical transmittance from 71.9 % to 79.3 % at 550 nm and decreased the sheet resistance from 11.4 ohm sq^{-1} to 9.8 ohm sq^{-1}, but also improved the adhesivity of AgNW network on FTO substrate. Furthermore, MnO_2 nanosheets were directly deposited on welded-AgNW/FTO (wAF) substrate to prepare a transparent MnO_2/weled-AgNW/FTO (MwAF) composite electrode. The MwAF electrode displayed excellent electrochemical performance, including high specific capacitance (375 F g^{-1} at 5 mV s^{-1}) and superior cycle stability (173.3 % of the initial capacitance after 20000 GCD cycles).

Keyword: silver nanowires, welding treatment, transparent, MnO_2, supercapacitors

1. Introduction

Transparent conductive electrodes (TCEs) due to high conductivity and high transparency have been widely used as the critical components of many optoelectronic devices, like solar cells, light-emitting diodes (LEDs), touch screen panels, and plasma displays [1-5]. In general, tin doped indium oxide (ITO) is the most widely used TCE material in these applications because of its excellent electrical conductivity and optical transmittance. However, ITO is subject to some drawbacks such as scarcity and high cost of indium, inherent brittleness, and the high temperature processing to restrict its practical applications. Therefore, various transparent electrodes, like carbon nanotubers (CNT), graphene, conducting polymers, and metal nanowires mesh, have been investigated to replace ITO [3,6].

Ag nanowires (AgNW) network has attracted considerable attention as one of the most promising candidates due to high transparency, excellent conductivity, good mechanical flexibility, high surface area, and solution process-ability [7]. Moreover, large-scale and high-yield synthesis of AgNW has been achieved using polyol reduction methods. However, for practical application of AgNW film, there are several issues that need to be addressed. Firstly, the AgNW-AgNW contact resistance is too large because of the insulating coating of polyvinylpyrrolidone (PVP) on the surface of AgNW and the

loose contact at the crossed section of AgNWs [8,9]. Several post-processes such as mechanical pressing, fast light sintering, and thermal annealing, have been required to decrease the resistance of AgNW network [10]. Secondly, AgNW network is easy to fall off owing to poor adhesion between AgNW and substrates [11]. For the initial AgNW network, the connections at the crossed section are mainly via physical contacts, such as van der Waals forces and capillary force form solvent evaporation.[12] Therefore, the formation of junction contacts at the crossing points of AgNWs and between AgNW and substrate on surface of AgNW can effectively improve the mechanical adhesion[13]. Brongersma and co-workers demonstrated a light-induced plasmonic nano-welding technique to achieve welding together AgNW selectively at junction points [5]. Recently, our group also reported that a fluorine doped ZnO_2 (FZO) layer coating on surface of AgNW, which not only decreased sheet resistance of AgNW network but also provided strong adhesion and weld [14].

In the paper, the optical transmittance and conductivity of AgNW/F-doped SnO_2 (FTO) conducting film were improved by a post-process method. For this purpose, we developed a facile polyol method to prepare AgNW with high aspect ratio, which were spin-coated on surface of FTO to form AgNW/FTO conducting film. Then, the AgNW/FTO conducting film was welded to form junctions using a rapid annealing process, which increased the optical transmittance from 71.9 % to 79.3 % at 550 nm and reduced the sheet resistance from 11.4 ohm sq^{-1} to 9.8 ohm sq^{-1}. Moreover, we adopted welded-AgNW/FTO (wAF) conducting film to prepare transparent MnO_2/weled-AgNW/FTO (MwAF) composite electrodes, which exhibited excellent capacitive performance with high specific capacitance (375 F g^{-1} at 5 mV s^{-1}) and superior cycling stability (~173.3 % after 20000 cycles).

2. Experimental

2.1. Synthesis of AgNW and preparation of Ag NW network

The silver nanowires with high aspect ratio were synthesized using a new polyol process. During the synthesis, 0.34 g of polyvinylpyrrolidone (PVP) with high molecular weight (*Mw*≈1300000) was dissolved into a 15 mL ethylene glycol (EG) solution of 0.1mM $FeCl_3$ and heated to 170^{o}C, and was named as solution A. Next, 0.16 g of $AgNO_3$ was added to 5 mL EG solution and stirred to uniformity as Solution B. Then, 30 mg of $AgNO_3$ was added into the Solution A stirred for initial nucleation of the silver seeds. After 5 min, the Solution B was injected into the Solution A drop by drop using a syringe within 10 min. The mixed solution was allowed to react for 30 min. The cooled solution at room temperature was centrifuged five times at 9000 rpm. Then, the AgNW/ethanol solution was spun on the surface of FTO substrates at a 3000 rpm for several times to prepare the AgNW/FTO conducting films. Finally, the AgNW/FTO conducting films were welded by a rapid thermal annealing process for 30 min by the rate of 40 °C/s and then cooled down naturally under Ar atmosphere.

2.2. Preparation of transparent MwAF composite electrodes

The transparent MwAF composite electrodes were fabricated by an electrochemical deposition technology. The carbon, saturated calomel and welded-AgNW/FTO conducting films were as the counter electrode, reference electrode and working electrode, respectively. The electrolyte was the mixture of 0.1 M $Mn(CH_3COO)_2$•$4H_2O$ and 0.1 M Na_2SO_4, and its pH was set to 6 by adding dilute H_2SO_4. The MnO_2 nanosheets were deposited onto the welded-AgNW/FTO (wAF) conducting films in potentiostatic mode under 0.45 V for 400s to fabricate the transparent MwAF composite electrodes. Finally, the composite electrodes were washed in distilled water.

2.3. Characterization

Morphology and crystal structure studies of the samples were performed with a field emission scanning electron microscope (SEM, Quanta 250, FEI), and X-ray diffraction (XRD, D8-Advance, Bruker), respectively. The transmittance spectra were measured using a UV-vis-NIR spectro-photometer (UV-3600, Shimadzu) equipped with an integrating sphere. The sheet resistances were measured by a four-point probe method with a source/meter (Keithley 2162A) and probe station

(ECOPIA, ESP300). Cyclic voltammetry (CV), Galvanostatic charge/discharge (GCD) and electrochemical impedance spectroscopy (EIS) were carried out in a three-electrode system using an electrochemical workstation (Zahner/Zennium E 6.0). The electrolyte was a 0.5 M Na_2SO_4 aqueous solution.

3. Results and discussion

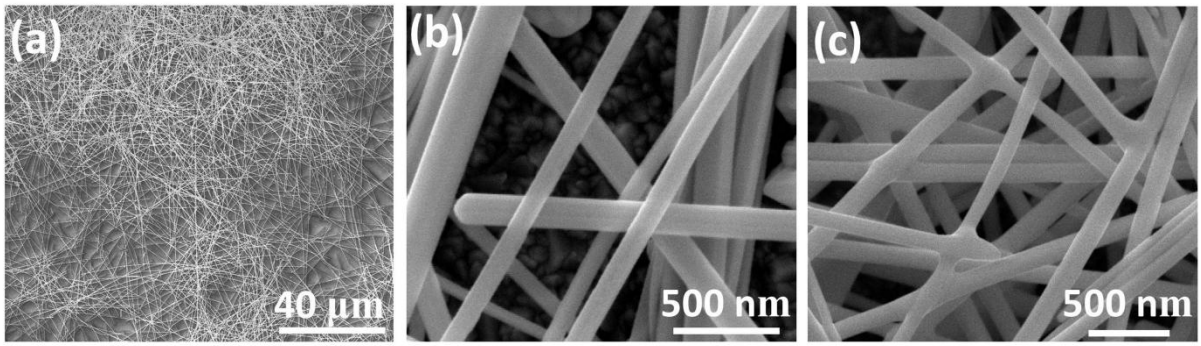

Figure 1. (a) (b) SEM images of AgNW networkand, (c) the weldled-AgNW/FTO conducting film.

Figure 1(a) and 1(b) show the typical SEM images of the AgNW/FTO conducting film before annealing treatment. The diameters of these as-grown AgNW are about 50 to 200 nm and the lengths are about 40 to100 μm. However, the initial AgNW network is easy to loose or peel off due to the connections at the crossed section by physical contacts, like van der Waals forces and capillary force form solvent evaporation[14].Then, the AgNW/FTO conducting film is welded by annealing process, and the welding points at the crossing points of AgNWs are clearly observed, as shown in figure 1(c). Importantly, away from each junction the nanowires are unaffected by the annealing treatment and no further morphological changes were observed.

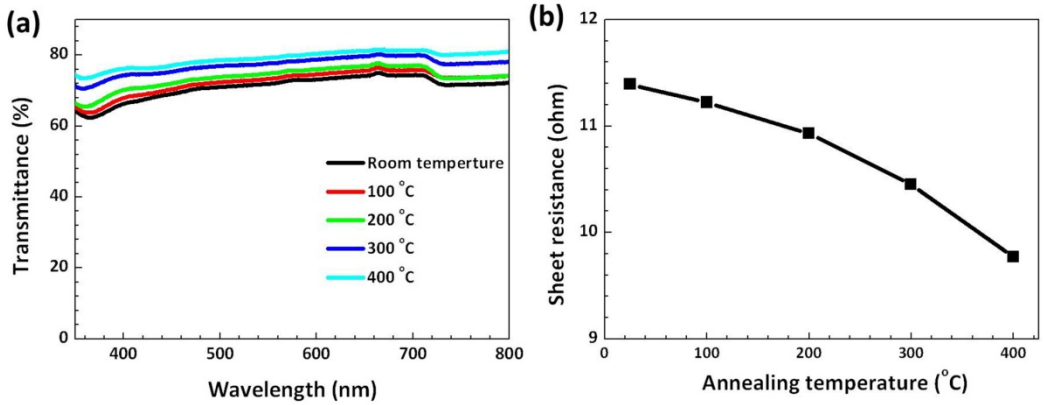

Figure 2. (a) the optical transmittance spectra of the same AgNW/FTO conducting film and (b) the corresponding sheet resistances at different annealing temperature.

To investigate the photoelectric properties of AgNW/FTO conducting film, the same AgNW/FTO conducting film is annealed at various temperatures, respectively. In figure 2(a) and 2(b), the optical transmittance of the as-prepared AgNW/FTO conducting film is only about 71.9 % at 550 nm, and the corresponding sheet resistance is 11.4 ohm sq^{-1}. Then, the AgNW/FTO conducting film is welded by a rapid thermal annealing process. With increasing annealing temperature, its sheet resistances gradually decrease and the corresponding optical transmittances increase. When the annealing temperature is up to 400 ^{o}C, the optical transmittance increases to 79.3 % at 550 nm and the sheet resistance reduces to

9.8 ohm sq^{-1}.On the one hand, the more welding points of AgNWare formed to decrease the sheet resistance of AgNW network with increase the annealing temperature; on the other hand, the whole thickness of AgNW network can become thinner to increase the optical transmittance due to the top Ag nanowires into the bottom Ag nanowires by welding process.

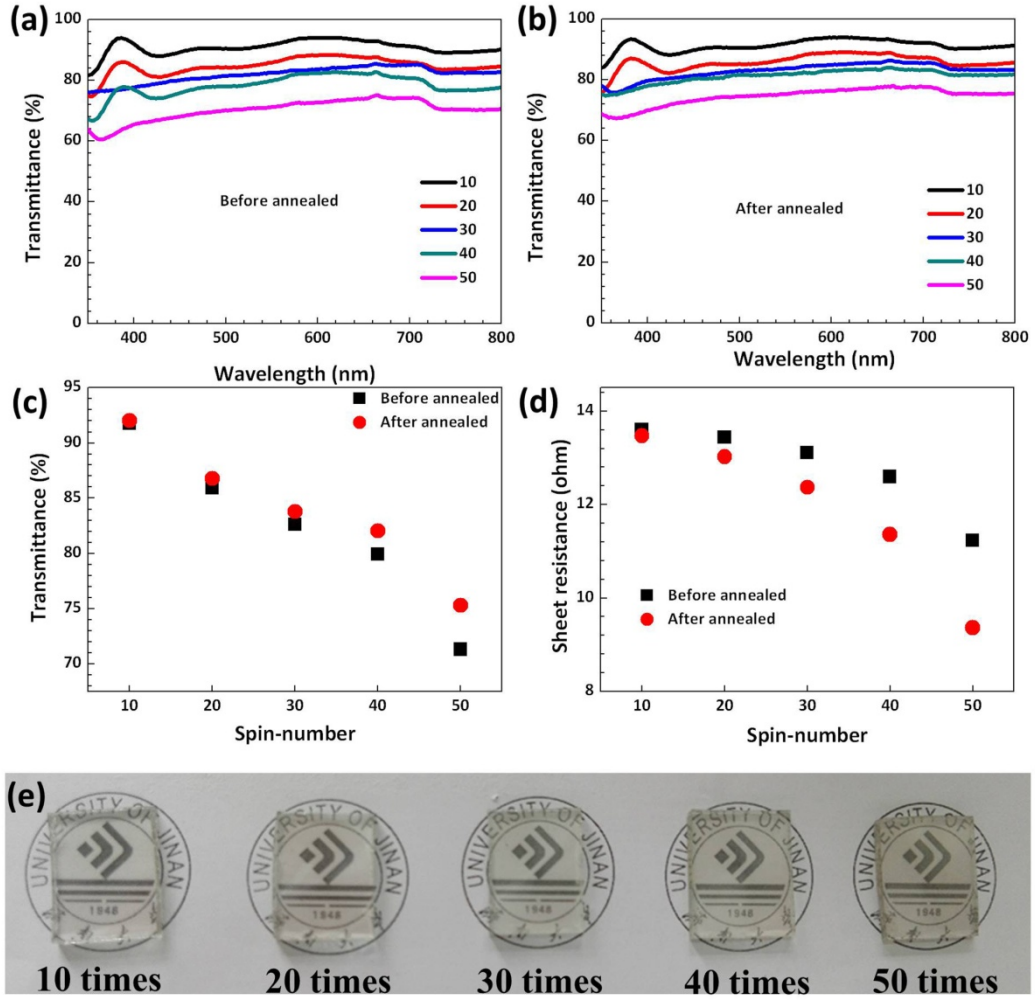

Figure 3. (a) optical transmittance spectra of AgNW/FTO conducting films with different spin-number before and (b) after annealing process, (c) transmittance versus spin-number for AgNW/FTO conducting films, (d) sheet resistances versus spin-number for AgNW/FTO conducting films, (e) A photograph of the weld-AgNW/FTO conducting films with different spin-coating numbers of AgNW ink .

Figure 3 shows the effect of annealing treatment on the optical transmittance and sheet resistance of the AgNW/FTO conducting films with different spin-number of AgNW ink. As shown in figure 3(a) and 3(b), the transmittances of AgNW/FTO conducting films decrease with the increase of AgNW spin-coating times before and after annealing process. Figure 3(c) shows the optical transmittance of the AgNW/FTO conducting film before and after annealing treatment. The transmittance of the as-prepared AgNW/FTO conducting film at 550 nm reaches 91.8 % when the spin-coating number is 10 times; 85.9 % at 20 times, 82.6 % at 30 times, 79.9 % at 40 times, and 71.3 % at 50 times. After annealing treatment, their transmittance increase to 92 %, 86.8 %, 83.8 %, 82.1 %, and 75.3 %, respectively. In figure 3(d), the sheet resistance of the AgNW/FTO conducting film is about 13.6 $ohmsq^{-1}$ at 10 spin-coating times before annealing. With increasing to 50 times, the resistance sheet

reduces to 11.2 ohm sq^{-1}. Then, the AgNW/FTO conducting films are welded at 400°C. Compared with as-prepared AgNW/FTO conducting films, the decreases of sheet resistance for the wAF conducting films are even more obvious with increasing the number of spin-coating. For instance, the sheet resistance decreases from 11.2 to 9.4 ohm sq^{-1} at spin-coating times of 50 after annealing process while the sheet resistance only decreases by 0.1 ohm sq^{-1} at 10 times. Figure 3(e) shows the photograph of the wAF conducting films with different spin-coating times of AgNW/FTO conducting films.

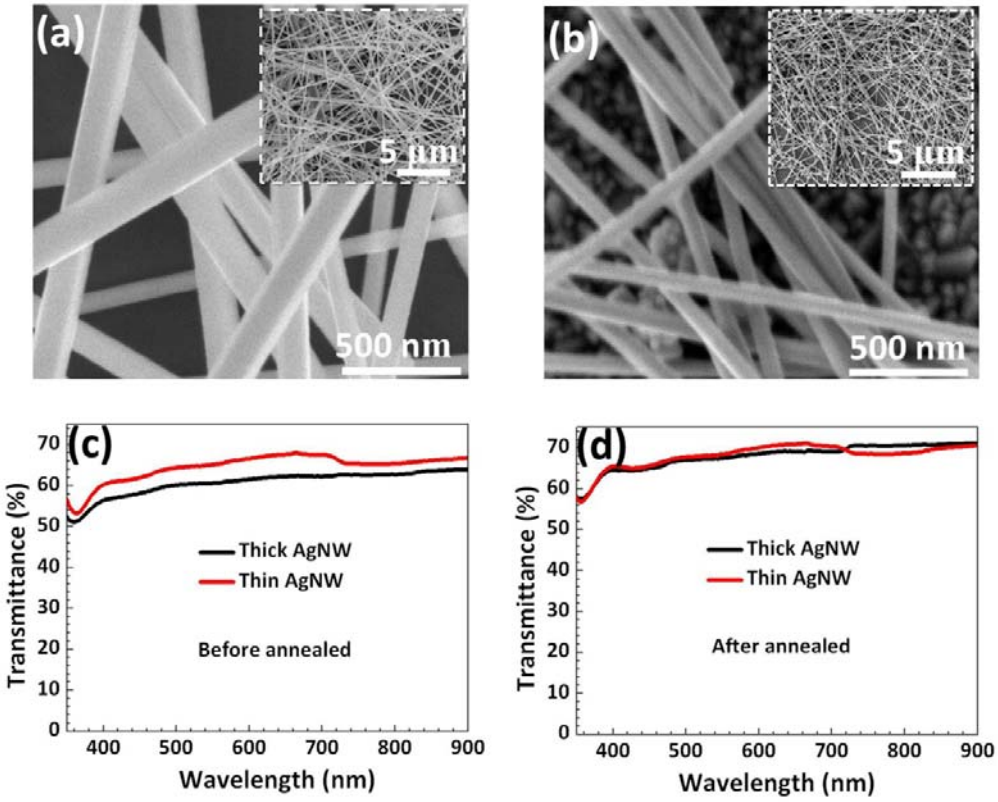

Figure 4. (a) SEM images of thethick AgNW/FTO conducting film and (b) thin AgNW/FTO conducting film at 5.7 ohm sq^{-1}, (c) The corresponding transmittance spectra of thick and (d) thin AgNW/FTO conducting films before annealing treatment and after annealing treatment.

The Ag nanowires with different diameter and length can be obtained by the control of growth time. Figure 4(a) and 4(b) show the SEM images of thick and thin AgNW/FTO conducting films at 5.7 ohm aq^{-1}, and their diameter are about 170 nm and 80 nm, respectively. AgNW network of the two samples distribute uniformly on FTO substrates. However, the holes of the thin AgNW films are more than that of the thick AgNW films (see the insets of figure 4(a) and 4(b)). As shown in figure 4(c), the transmittances of as-prepared thick AgNW/FTO conducting film are 60.6 % at 550 nm while that of the as-prepared thin AgNW/FTO conducting film are 65.1 %, indicating the greater optical transmittance of as-prepared thin AgNW/FTO conducting film. Then, the samples were carried out annealing treatment, and their optical transmittance spectra are displayed in figure 4(d). The thick AgNW/FTO conducting film shows a transmittance of 67.5 % after annealing, giving 6.9 % difference from the initial value, while the thin AgNW/FTO conducting film with initial transmittance of 65.1 % becomes only 3.3 % more transparent after annealing treatment.

AgNW/FTO conducting film with unique properties like good electrical conductivity, high specific surface area, and high transmittance, can be applied to transparent supercapacitors as an ideal current collector material. In our paper, MnO_2 is directly grown on wAF conducting film using electrochemical deposition method to prepared flower-like transparent MwAF composite electrodes.

Figure 5(a) and 5(b) clearly show that MnO_2 nanosheets are uniformly coated on the wAF conducting film. The MwAF composite electrodes have large surface area, which can give sufficient the electrochemical active sites to enhance the capacitive performance [15]. Figure 5(c) shows the XRD pattern of the transparent MwAF composite electrode. The diffraction peaks at about 38.1°, 44.3°, 64.4° and 77.5° are observed, which can be assigned to the (111), (200), (220), and (311) planes of metallic Ag (JCPDFS 04-0783). The peak at 32.3° is the characteristic peaks of AgO (JCPDFS 43-1038). The peaks at 26.5°, 33.8°, 37.8°, 51.6°, 61.7°, and 65.7° can demonstrate the presence of cassiterite SnO_2 (JCPDFS 77-0451) from the FTO film. The diffraction peaks at 26.6°, 34.0°, 37.9°, and 54.8° are observed, which correspond to the (201), (301), (111), and (402) reflections ramsdellite MnO_2 (JCPDFS 42-1316), respectively, supporting the successful preparation of MwAF composite in our samples. Figure 5(d) shows the MwAF composite electrode, and its transmittance is about 23.8 % at 550 nm. According to the inset of figure 5(d), the brown electrode material is a transparent film, and can make the words in the background clearly visible.

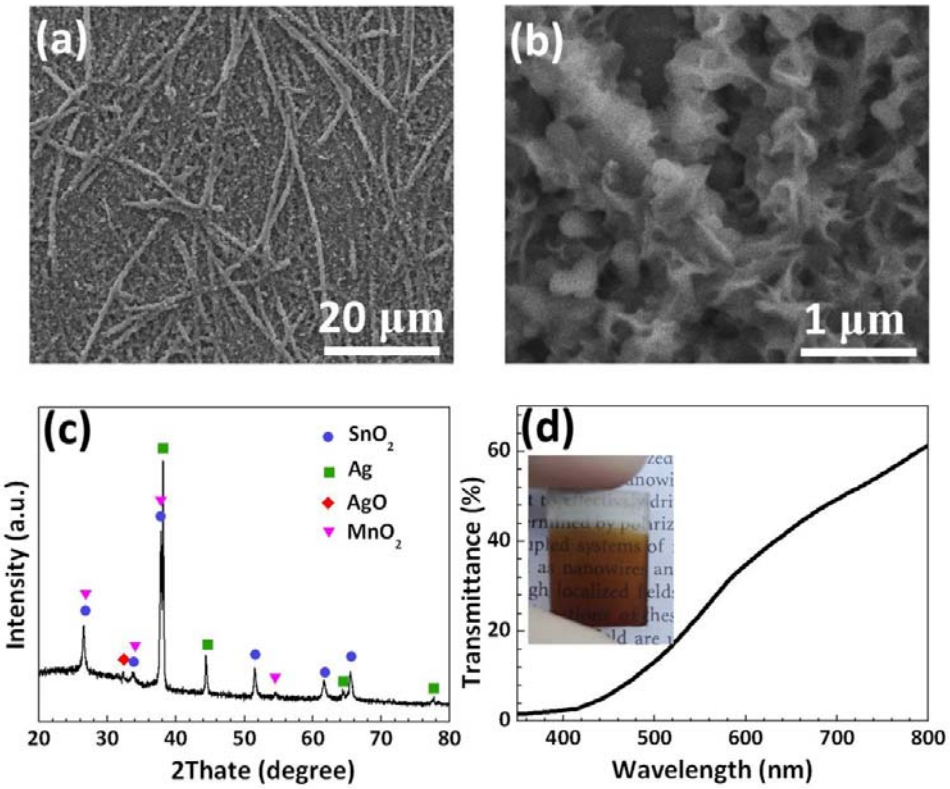

Figure 5. (a) and (b) SEM image of the MwAF electrode, (c) XRD pattern of the MwAF electrode, (d) optical transmittance spectra of the MwAF electrode, the inset is a photograph of the MwAF composite electrode.

To further evaluate the capacitive properties of the transparent MwAF composite electrodes, electrochemical studies are conducted in a three-electrode cell in 0.5 M Na_2SO_4 electrolytes. Figure 6(a) shows CV curves of the MwAF composite electrode at different scan rates. The shapes of the CV curves are roughly rectangular mirror images characteristic, which indicates ideal capacitive behaviour and good high-rate capability [16, 17]. Figure 6(b) displays the variation in the specific capacitance of the MwAF electrode as a function of the scan rate. The specific capacitance of the MwAF electrode are up to 375, 286, 218, 177, 142, and 110 F g^{-1} at scan rates of 5, 10, 25, 50, 100, and 200 mVs^{-1}, respectively. The good capacitive performance of the MwAF electrode is mainly due to both the larger surface area of flower-like architectures MnO_2 layer and excellent conductivity of AgNW network. Figure 6(c) shows the cycling stability of the MwAF electrode, which is achieved via conducting GCD

cycling at a current density of 7 Ag^{-1}.The specific capacitance of the MwAF electrode continuously increases in the initial cycles, which is due to the electrochemical active process of electrodes [18, 19]. During the first 5000 cycles, its specific capacitance increases from 191.1 F g^{-1} to 312 F g^{-1}, showing an 170 % retention. Until 10000 cycles, the specific capacitance of the MwAF electrode reaches the maximum value, 181 % of its initial capacitance. After 20000 cycles, the MwAF electrode still remains at 173.3 % of its initial capacitance, demonstrating its excellent long-term cycling stability. The inset of figure 6(c) is the GCD curves at different current densities from 3.5 to 28 A g^{-1}, which are linear and symmetrical charge and discharge profiles, indicating good super-capacitive behaviour of the MwAF electrode. The electrochemical performance of the MwAF electrode is further studied by electrical impedance spectroscopy (EIS) measurement, and the Nyquist plot is shown in figure 6(d). A small charge transfer resistance of the MwAF electrode is confirmed by the small diameter of the semicircleof 34.1 ohm, which is lower than that of the pure MnO_2, indicating that the MwAF composite electrode has a good capacitance behaviour [20].

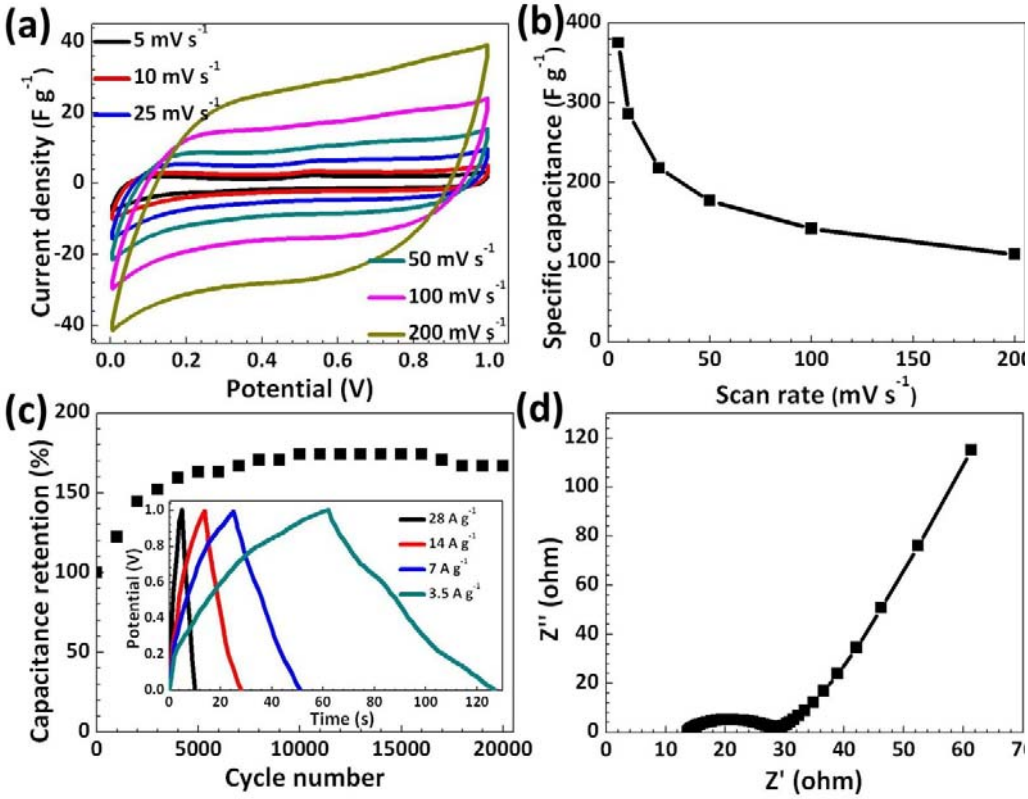

Figure 6. (a) CV curves of the MwAF electrode at different scan rates, (b) Specific capacitance of the MwAF electrode at different scan rates, (c) Cycling performance of the MwAF electrode at current density of 7 A g^{-1}, the inset is the GCD curves at different current densities, (d) EIS curves of theMwAF electrode.

4. Conclusion

We have demonstrated a facile and novel polyol method to prepare AgNW with high aspect ratio. The AgNW/FTO conducting film is then obtained by spin-coating, which presents good optical transmittance with 71.9 % at 550 nm and low sheet resistance with 11.4 ohm sq^{-1}. Then, welding treatment using a rapid annealing process for AgNW/FTO conducting film form welding junctions at AgNW crossing points, which canimprove the transmittance to 79.3 % and decrease the sheet resistance to 9.8 ohm sq^{-1}. Furthermore, the wAF film shows good adhesivity of AgNW network and high surface area. Based on the unique properities, we also prepared transparent MwAF composite as

a supercapacitor electrode. The transparent MwAF composite electrode not only has large surface area, but also shows high specific capacitance with 375 F g^{-1} at 5 mV s^{-1}, and good cycle stability with 173.3 % retention after 20000 cycles. This study provides a new route for the application and development of AgNW in future optoelectronic and energy storage devices.

Acknowledgement
This work is supported by the National Natural ScienceFoundation of China (No. 11404138, 51401239, 21477047),Shandong Provincial Natural Science Foundation of China(No. BS2014CL019, ZR2013BL002).

References
[1] Sukanta D, Thomas M, Philip E, Evelyn M, Peter N, Werner J, John J and Jonathan N 2009 *ACS nano* **3**17
[2] Gaynor W, Burkhard G, McGehee M and Peumans P 2011 *Adv.Mater.* **23** 2905
[3] Kim T, KimY, LeeH, Kim H, Yang W and Suh K 2013 *Adv.Funct. Mater.* **23** 1250
[4] Selzer F, Floresca C, Kneppe D, Bormann L, Sachse C, Weiß N, Eychmüller A, Amassian A, Müller-Meskamp L and Leo K 2016 *Appl. Phys. Lett.* **108** 163302
[5] Garnett E, Cai W, Cha J, Mahmood F, Connor S, Greyson C, Cui Y, McGehee M and Brongersma M 2012 *Nat.Mater.* **11** 241
[6] Im H, Jin J, Ko J, Lee J, Lee J and Bae B 2014 *Nanoscale* **6** 711
[7] Oh H and Lee M 2016 *Mater. Lett.* **176** 110
[8] Lee J, Lee I, KimT and Lee J 2013 *Small* **9** 2887
[9] Jin Y, Deng D, Cheng Y, Kong L and Xiao F 2014 *Nanoscale* **6** 4812
[10] Weiß N, Müller-Meskamp L, Selzer F, Bormann L, Eychmüller A, Leo K and Gaponik N 2015 *RSC Adv.* **5** 19659
[11] Zhu, Chung C, Cha K, Yang W, Zheng Y, Zhou H, Song T, Chen C, Weiss P, Li G and Yang Y 2011 *ACS nano* **5** 9877
[12] Qiao Z, Yang X, Yang S, Zhang L and Cao B 2016 *Chem. Commun.* **52** 7998
[13] Nian Q, Saei M, Xu Y, Sabyasachi G, Deng B, Chen Y and Cheng G 2015 *ACS nano* **9** 10018
[14] Han J, Yuan S, Liu L, Qiu X, Gong H, Yang X, Li C, Hao Y and Cao B 2015 *J. Mater. Chem. A* **3** 5375
[15] Chi H, LiY, Xin Y and Qin H *Chem. Commun.* **50** 13349
[16] Lang X, Hirata A, Fujita T and Chen M 2011 *Nat.Nanotechnol.* **6** 232
[17] Lu X, Zheng D, Zhai T, Liu Z, Huang Y, Xie S and Tong Y 2011 *Energy Environ. Sci.* **4** 2915
[18] Liu Z, Xu K, Sun H and Yin S 2015 *Small* **11** 2182
[19] Yu M, Zeng Y, Han Y, Cheng X, Zhao W, Liang C, Tong Y, Tang H and Lu X 2015 *Adv. Funct. Mater.* **25** 3534
[20] Xia H, Hong C, Shi X, Li B, Yuan G, Yao Q and Xie J 2015 *J. Mater. Chem. A* **3** 1216